

Mathematical Biosciences 164 (2000) 17-38

# Mathematical Biosciences

www.elsevier.com/locate/mbs

### A mathematical model to study the effects of drug resistance and vasculature on the response of solid tumors to chemotherapy

Trachette L. Jackson a,\*, Helen M. Byrne b

a Department of Mathematics, Duke University, P.O. Box 90320, Durham, NC 27708-0320, USA
 b Division of Theoretical Mechanics, School of Mathematical Sciences, University of Nottingham, Nottingham NG7 2RD, UK

Received 15 June 1999; received in revised form 22 November 1999; accepted 23 November 1999

#### Abstract

A mathematical model is developed that describes the reduction in volume of a vascular tumor in response to specific chemotherapeutic administration strategies. The model consists of a system of partial differential equations governing intratumoral drug concentration and cancer cell density. In the model the tumor is treated as a continuum of two types of cells which differ in their proliferation rates and their responses to the chemotherapeutic agent. The balance between cell proliferation and death within the tumor generates a velocity field which drives expansion or regression of the spheroid. Insight into the tumor's response to therapy is gained by applying a combination of analytical and numerical techniques to the model equations. © 2000 Elsevier Science Inc. All rights reserved.

Keywords: Mathematical model; Vascular tumors; Chemotherapy

#### 1. Introduction

Over the past two decades, solid tumor growth has been fertile ground for mathematical modeling and many such models have appeared in the literature [1–9]. Guided by in vitro experiments involving clusters of tumor cells which are termed multicellular spheroids, the majority of these models focus on the avascular stage of tumorigenesis and view the tumor as a spherical mass of cancer cells which are either proliferating, quiescent or dead. Most of the dead cells are

0025-5564/00/\$ - see front matter © 2000 Elsevier Science Inc. All rights reserved.

PII: S0025-5564(99)00062-0

<sup>\*</sup>Corresponding author. Fax: +1-919 660 2821.

E-mail address: tjackson@math.duke.edu (T.L. Jackson).

concentrated in a central necrotic core in which the concentration of vital nutrients is insufficient to sustain live cells. The necrotic core is surrounded by an annulus containing predominantly live cells and isolated cells undergoing natural or programmed cell death. The nutrient concentration increases steadily from the inner to the outer edge of this annulus. Consequently cells towards the inner boundary are quiescent (they have sufficient nutrient to remain alive but insufficient to proliferate) whilst those towards the tumor boundary proliferate rapidly [10–12]. Many of the existing models are comprised of an integro-differential equation describing the temporal evolution of the tumor boundary and reaction–diffusion equations governing intratumoral distributions of vital nutrients and growth-inhibitory factors [1–8].

In this study, the response of a vascular tumor to chemotherapeutic treatment is discussed. Particular attention is paid to the effect that the incorporation of a semi-resistant tumor cell type has on the tumor's overall growth dynamics. To date mathematical models of vascular tumor growth have neglected their spatial heterogeneity and treated the tumor as a spatially-uniform mass which evolves at some prescribed rate such as logistic or Gompertzian. For example, Marusic et al. [13] compared the ability of 14 spatially-uniform mathematical models to capture the in vivo volume growth of two murine tumor cell lines. By contrast to [13], here we derive a spatially-dependent mathematical model for vascular spheroid growth based firmly on the underlying biology. Our work differs from that of other authors who have developed spatio-temporal models [1–9] in that there is no explicit mention of a diffusible nutrient; instead, equations are derived that describe the evolution of the tumor volume, the different types of cancer cells that it contains and the externally-supplied drug. We adopt a modeling approach similar to Byrne and Chaplain [4] to describe the vascular transfer of drug between the blood and tumor. Where they considered the constant transfer of nutrient from the vasculature, we study the spatially-dependent transfer of chemotherapeutic drugs into and out of the tumor. Parameter values are taken from published data on nude mice treated with the anti-cancer agent doxorubicin. Whilst the inclusion of cell densities renders the model similar to that of Ward and King [9], several features distinguish this work. For example, Ward and King's model describes avascular tumor growth in response to an externally-supplied nutrient whereas we are concerned with the effect that bloodborne delivery of chemotherapeutic drugs has on the growth of vascular tumors which may contain several subpopulations whose responses to the therapy differ.

When only one cell type is present, this modeling approach allows for the analytical estimation of the minimum tumor radius that is achieved after a bolus injection of a single blood-borne agent; as well as the time of tumor re-growth. We can also derive an equation for the largest tumor that can be eradicated by this type of treatment. When a semi-drug resistant cell population also inhabits the tumor, although the speed of the tumor's recovery is virtually unchanged, tumor reduction is significantly decreased, leading to a much increased time of cure when the tumor is exposed to a continuous infusion of the drug.

Although this model describes the way in which vascular tumors respond to traditional chemotherapy, it is our intention to extend the model to study tumor response to new two-step drug targeting strategies. Jackson and coworkers [14,15] present a detailed mathematical study of antibody–enzyme conjugates for the activation of anti-cancer prodrugs. The models are able to predict intratumoral and systemic concentrations of conjugate, prodrug and drug. Validation of the model is provided by experiments with the L49-sFv-bL fusion protein/cephalosporin doxorubicin system in nude mice bearing 3677 human melanoma xenografts. There have also been

experimental studies of tumor reduction due to this type of treatment which could be used to validate our modified mathematical model.

The outline of the paper is as follows. In Section 2 we present our mathematical model. In Section 3 we discuss a simplified version of the model, in which the tumor contains only one type of drug sensitive cell. The corresponding numerical and analytical results not only provide us with insight into the behavior of the model but also act as a useful benchmark for comparison with results presented in Sections 4 and 5 which pertain to tumors containing a drug sensitive and a drug resistant cell population. A summary of the key results is presented in the concluding Section 6, together with a discussion of their implications for cancer treatment.

#### 2. Model development

The goal of this study is to develop a deterministic model that describes tumor reduction due to blood-borne chemotherapy. The tumor is viewed as a densely packed, radially-symmetric sphere of radius R(t) containing two cell types: a rapidly dividing population  $p(\mathbf{r},t)$  (# of cells per mm³) that is highly susceptible to the drug; and a population  $q(\mathbf{r},t)$  (# of cells per mm³) that has lower drug susceptibility. Cell movement is produced by the local volume changes that accompany cell proliferation and death. It is convenient to associate with such movement a local cell velocity  $\mathbf{u}(\mathbf{r},t)$ . The spheroid expands or shrinks at a rate which depends upon the balance between cell growth and division and cell death within the tumor volume, the latter term being modified by the presence of the drug,  $d(\mathbf{r},t)$ .

We exploit the spherical symmetry of the problem by assuming henceforth that the spatially-dependent variables p, q, d and **u** depend only on the radial distance from the center of the tumor, r, and time, t.

The governing equations for drug concentration and the two populations of tumor cells are derived by applying the principle of conservation of mass to each species and may be written as follows:

$$\frac{\partial d}{\partial t} + \nabla \cdot (\mathbf{u}d) = \nabla \cdot (D(r)\nabla d) + \Gamma(r)(d_B(t) - d) - \lambda d, \tag{1}$$

$$\frac{\partial p}{\partial t} + \nabla \cdot (\mathbf{u}p) = D_p \Delta p + F_p(p) - C_p(d, p), \tag{2}$$

$$\frac{\partial q}{\partial t} + \nabla \cdot (\mathbf{u}q) = D_q \Delta q + F_q(q) - C_q(d, q). \tag{3}$$

In Eq. (1), D(r) is the diffusion coefficient of the drug in the tumor tissue which may realistically depend upon r. The function  $d_B(t)$  is the prescribed drug concentration in the tumor vasculature and  $\Gamma(r)$  represents the rate coefficient of blood–tissue transfer. Like D(r),  $\Gamma$  may depend on radial position. Finally,  $\lambda$  denotes the rate of drug loss due to decay, molecular instability, or cellular uptake and metabolism. In Eqs. (2) and (3)  $D_p$  and  $D_q$  are the assumed constant random motility coefficients of the two types of tumor cells and  $F_p$  and  $F_q$  are their respective net proliferation rates (rate of natural cell death subtracted from the rate of cell division) in the absence

of therapy. The functions  $C_p$  and  $C_q$  represent the effect of the chemotherapy on each cell population. We remark that there is no coupling between the two cell populations in the cell proliferation rates or the drug-induced cell kill terms. The effect of such interactions will form the subject of further work.

We anticipate that, in general, the functions D(r) and  $\Gamma(r)$  will be non-decreasing functions satisfying  $D(r) \to D_0$  and  $\Gamma(r) \to \Gamma_0$  as  $r \to \infty$ . There is experimental evidence that both molecular diffusion and vascular transfer are lowest near the center of the tumor, increasing to maximal levels at the tumor periphery [16,17]. The functions  $F_p(p)$  and  $F_q(q)$  are generally bounded functions of cell density satisfying  $F_p(0) = F_q(0) = 0$ . Finally, we assume that the functions  $C_p$  and  $C_q$  satisfy Michaelis-Menten kinetics and can be written in the general form  $C_i(d,x) = \beta_i dx/(\gamma_i + x)$  for positive parameters  $\beta_i, \gamma_i$  (i = p,q).

In order to obtain an equation for the velocity,  $\mathbf{u}$ , we assume that there are no voids within the tumor, that the proportion of the spheroid occupied by tumor cells remains constant, and that the proportion of vascular space within the tumor remains constant. Using these assumptions, it follows that q can be expressed in terms of p via the relation

$$p+q=k\equiv {\rm constant}.$$
 (4)

Adding Eqs. (2) and (3), and using (4) to eliminate q, leads to the following equation for the local velocity:

$$k\nabla \cdot \mathbf{u} = (D_p - D_q)\Delta p + F_p(p) + F_q(k-p) - C_p(d,p) - C_q(d,k-p). \tag{5}$$

Eqs. (1), (2) and (5) are sufficient to determine the intratumoral drug concentration d, the cell density p, and the radial component of the velocity vector  $\mathbf{u}$ .

In order to assess the tumor's response to the chemotherapeutic treatment it will be important to follow the evolution of the tumor volume (=  $(4/3)\pi R^3$ , for radial symmetry), or equivalently, the tumor radius R(t). We do this by noting that, under radial symmetry, the tumor expands at a rate which is equal to the radial component of the velocity there, that is

$$\frac{\mathrm{d}R}{\mathrm{d}t} = u(R(t), t). \tag{6}$$

To complete this system we impose the following initial and boundary conditions:

$$R(0) = R_0, \quad p(r,0) = p_0(r), \quad d(r,0) = 0, \quad d_B(0) = d_0,$$
 (7)

$$\frac{\partial d(0,t)}{\partial r} = 0, \quad d(R(t),t) = d_N(t), \quad u(0,t) = 0,$$
(8)

$$\frac{\partial p}{\partial r}(0,t) = \frac{\partial p}{\partial r}(0,t) = 0,$$
(9)

$$D_{p}\frac{\partial p}{\partial r}(R,t) - u(R,t)p(R,t) = 0, \quad D_{q}\frac{\partial q}{\partial r}(R,t) - u(R,t)q(R,t) = 0.$$

$$(10)$$

These conditions imply that we begin with a tumor of given initial cell density and radius,  $R_0$ . We also assume that there is no drug in the tumor tissue at time zero, but that there is an initial constant concentration of drug in the tumor vasculature at that time. By symmetry, at r = 0 there

is no flux of drug and the local velocity is zero. The concentration of drug on the tumor boundary is assumed to be equal to  $d_N(t)$ , the drug concentration in the surrounding normal tissue. Finally, for the two cell populations, we impose no flux of p and q at the tumor center and on its outer boundary.

#### 2.1. Non-dimensionalization

We re-scale our mathematical model in the following manner, denoting non-dimensional variables with bars:

$$d = d_0 \bar{d}, \quad u = R_0 \alpha \bar{u}, \quad p = k \bar{p}, \quad t = \frac{1}{\alpha} \bar{t}, \quad r = R_0 \bar{r}, \quad \epsilon = \frac{\alpha R_0^2}{D}, \quad \bar{\lambda} = \frac{\lambda R_0^2}{D}, \quad \bar{\Gamma} = \frac{\Gamma R_0^2}{D}, \quad \bar{\beta}_i = \frac{\beta_i d_0}{\alpha}, \quad \bar{\gamma}_i = \frac{\gamma_i}{k}, \quad \sigma_1 = \frac{D_p}{R_0^2 \alpha}, \quad \sigma_2 = \frac{(D_p - D_q)}{\alpha R_0^2},$$

where  $\alpha_1$  is the inverse of the doubling time of untreated tumors [18] assumed to have only one cell type. After dropping bars for notational convenience, the resulting system of equations to be solved is

$$\epsilon \left\{ \frac{\partial d}{\partial t} + \nabla \cdot (\mathbf{u}d) \right\} = \nabla \cdot (D(r)\nabla d) + \Gamma(d_B(t) - d) - \lambda d, \tag{11}$$

$$\frac{\partial p}{\partial t} + \nabla \cdot (\mathbf{u}p) = \sigma_1 \Delta p + F_p(p) - C_p(d, p), \tag{12}$$

$$\nabla \cdot (\mathbf{u}) = \sigma_2 \Delta p + F_p(p) + F_q(1-p) - \frac{\beta_1 dp}{\gamma_1 + p} - \frac{\beta_2 d(1-p)}{\gamma_2 + 1 - p},\tag{13}$$

$$\frac{\mathrm{d}R}{\mathrm{d}t} = u(R(t), t),\tag{14}$$

$$R(0) = 1, \quad d(r,0) = 0,$$
 (15)

$$\frac{\partial d(0,t)}{\partial r} = 0, \quad d(R(t),t) = d_N(t), \quad u(0,t) = 0.$$
(16)

Inherent in this problem are two timescales: the tumor growth timescale ( $\approx 1$  day) and the much shorter drug diffusion timescale ( $R_0^2/D \approx 1$  min) [2]. Accordingly, the non-dimensionalization process introduces the small parameter  $0 < \epsilon = \alpha R_0^2/D \ll 1$  into the model equations. Also, since the diffusion coefficients of the cells,  $D_p$  and  $D_q$ , are much smaller than the diffusion coefficient of the much smaller and more motile drug molecules, D, the parameters  $\sigma_1$  and  $\sigma_2$  will be at most  $O(\epsilon)$ . We exploit the appearance of these small parameters in order to construct approximate solutions to Eqs. (11)–(16) which are valid in the limit as  $\epsilon, \sigma_1, \sigma_2 \to 0$ . We make use of published data for the treatment of nude mice with the anti-cancer drug doxorubicin. Table 1 lists each parameter, its baseline value, and source.

Table 1 List of baseline parameter values used in simulations and their sources

Parameter	Value	Reference
$d_0$	6 mg/kg	[24]
$R_0$	0.4 cm	[24] <sup>a</sup>
α	$\frac{1}{7}  day^{-1}$	[18] <sup>b</sup>
λ	$\frac{1}{7} \text{ day}^{-1}$ 1.9 day $^{-1}$	[33] <sup>c</sup>
$\xi_1$	$60 \text{ day}^{-1}$	[38]
$\xi_2$	$6 \text{ day}^{-1}$	[38] <sup>d</sup>
D	$1.7 \text{ cm}^2 \text{day}^{-1}$	[34] <sup>e</sup>
β	$560 \text{ M}^{-1} \text{day}^{-1}$	[35]e
Γ	$16 \text{ day}^{-1}$	[37] <sup>f</sup>

<sup>&</sup>lt;sup>a</sup> Kerr et al. (1996) began chemotherapeutic treatment when tumor volume was approximately 150 mm<sup>3</sup> ( $R_0 \approx 3.4$  mm) we chose the slightly larger initial tumor size of  $R_0 \approx 4$  mm.

#### 3. One cell type

In order to gain some insight into its behavior, we start by considering a simplified version of the governing equations. The reduced model is obtained by making the following additional assumptions:

- the tumor contains only one cell type, i.e. q=0;
- drug diffusion is spatially uniform, i.e. D(r) = D, constant;
- the rate of blood-tissue transfer is spatially uniform, i.e.  $\Gamma(r) = \Gamma$ , constant;
- in the absence of treatment (d=0) the net cell proliferation rate is governed by the logistic growth law so that  $F_p(p) = \alpha_1 p(1 (p/\delta_1))$ , where the positive constants  $\alpha_1$  and  $\delta_1$  are, respectively the proliferation rate and the carrying capacity in dimensional terms.

Under these assumptions Eqs. (11)–(13), when written in radially-symmetric coordinates, become

$$\epsilon \left\{ \frac{\partial d}{\partial t} + \frac{1}{r^2} \frac{\partial}{\partial r} (r^2 u d) \right\} = \frac{D}{r^2} \frac{\partial}{\partial r} \left( r^2 \frac{\partial d}{\partial r} \right) + \Gamma(d_B(t) - d) - \lambda d, \tag{17}$$

$$p = 1, (18)$$

$$\frac{1}{r^2}\frac{\partial}{\partial r}(r^2u) = 1 - \beta d,\tag{19}$$

where  $\alpha = \alpha_1(1 - (k/\delta_1))$  and  $\beta = \beta_1 k/(\gamma_1 + k)$ . We assume that  $\alpha, \beta > 0$  so that the tumor cells increase in number when no drug is present and the drug is effective at killing the tumor cells. Eqs. (17) and (19) together with (6)–(8) suffice to solve the problem.

<sup>&</sup>lt;sup>b</sup> Estimated from the growth of untreated tumors presented in Siemers et al. (1997).

<sup>&</sup>lt;sup>c</sup> Value used in Baxter et al. (1992) to study antibody metabolism.

<sup>&</sup>lt;sup>d</sup> There are no reports on the value of  $\xi_2$  for doxorubicin, we take  $\xi_2$  to equal to a tenth of the  $\xi_1$  reported in Robert et al. (1982).

<sup>&</sup>lt;sup>e</sup> Based on the internalization rate for doxorubicin reported in Dordal et al. (1992) and the assumption that approximately 10<sup>6</sup> must internalize to initiate cell death.

<sup>&</sup>lt;sup>f</sup> Estimated from the vascular permeability of doxorubicin used in Jain (1987).

#### 3.1. Analysis

To leading order, we solve Eq. (11) with  $\epsilon = 0$  and find

$$d(r,t) = \left(d_N(t) - \frac{\Gamma}{\xi^2} d_B(t)\right) \frac{R(t)\sinh\xi r}{r\sinh\xi R(t)} + \frac{\Gamma}{\xi^2} d_B(t),\tag{20}$$

where  $\xi^2 = \Gamma + \lambda$ . Substituting with (20) in (13) and integrating subject to u(0,t) = 0 leads to the following expression for the velocity in the tumor

$$u(r,t) = \left(1 - \frac{\beta \Gamma}{\xi^2} d_B(t)\right) \frac{r}{3} - \frac{\beta R(t)}{\xi^2} \left(d_N(t) - \frac{\Gamma}{\xi^2} d_B(t)\right) \frac{\xi r \cosh \xi r - \sinh \xi r}{r^2 \sinh \xi R(t)}.$$
 (21)

Finally, using (21) an ordinary differential equation which describes the temporal evolution of the tumor radius can be derived. Specifically, substituting (21) into (14) gives

$$\frac{\mathrm{d}R}{\mathrm{d}t} = \left(1 - \frac{\beta\Gamma}{\xi^2} d_B(t)\right) \frac{R}{3} - \frac{\beta}{\xi} \left(d_N(t) - \frac{\Gamma}{\xi} d_B(t)\right) \frac{\xi R \cosh \xi R - \sinh \xi R}{\xi R \sinh \xi R}.$$
(22)

The blood clearance data for many chemotherapeutic agents following a bolus injection can be fit quite nicely with an exponential or a bi-exponential function [14,15]. For this reason, we consider

$$d_B(t) = Ae^{-\xi_1 t} + Be^{-\xi_2 t}, d_N(t) = C(e^{-\xi_2 t} - e^{-\xi_1 t}),$$
(23)

where values for  $A, B, \, \xi_1$  and  $\xi_2$  can be obtained from experimental data. The normal tissue coefficient, C, is given by

$$C = \sqrt{k_{12}^2 + 2k_{12}k_e + 2k_{12}k_{21} + k_e^2 - 2k_{21}k_e + k_{21}^2/k_{12}}.$$

The parameters  $k_{12}$  and  $k_{21}$  are rates of transfer from the blood to the tissues of the body (including the tumor) and from the tissues back into the blood. In terms of the known blood clearance parameters we have  $k_{12} = AB(\xi_2 - \xi_1)^2/(A+B)^2$  and  $k_{21} = (A\xi_2 + B\xi_1)/(A+B)$  (see Appendix A for a derivation of these relations).

#### 3.1.1. Long time response

It is of interest to determine the long time behavior of the tumor in response to a bolus injection of a chemotherapeutic agent. As  $t \to \infty$ ,  $d \to 0$ ,  $u \to r/3$  and  $(dR/dt) \to R/3$ . This implies exponential growth of the tumor as a long time response to the treatment, i.e. the drug is ineffective on a long timescale because its decay and removal via the vasculature ensure that it eventually disappears from the tumor.

#### 3.1.2. Response of a small tumor

Analysis of Eq. (22) enables us to predict what dynamics will occur when treating a small tumor (this may refer to the final stages of treatment, after the drug has reduced the tumor to a sufficiently small size, or when there is early tumor detection so that the tumor is already small when treatment begins). When  $0 < R \ll 1$ , Eq. (22) reduces to  $(dR/dt) \sim (1 - \beta d_N(t))R/3$ , and exponential decay is predicted as long as  $d_N(t) > 1/\beta$ . At time  $t_c$  given by the solution of  $d_N(t_c) = 1/\beta$ ,

the tumor achieves its minimum radius,  $R_{\min}$ . If  $R_{\min}$  is sufficiently small that the continuum model is no longer valid, i.e.  $R_{\min} < R_c$ , we assume that the drug has forced the tumor into remission. This remission could lead to a cure or the cells could approach an avascular dormant state. However, if  $R_{\min} > R_c$ , we can estimate the time  $t_c$  at which the tumor will resume growth and the minimum radius achieved by assuming that in Eq. (23)  $\xi_2 \ll \xi_1$  (which is generally true of these experimentally determined parameters):

$$t_{\rm c} \sim -\frac{1}{\xi_2} \ln \frac{1}{\beta C} \approx 25.2 \text{ h},$$

$$R_{\rm min} \sim R_0 (\beta C)^{1/3\xi_2} e^{1/3\xi_2 (1-\beta C)} \approx 0.6R_0.$$
(24)

With parameters taken from Table 1, the time of relapse following a single bolus injection is approximately 25.2 h at which time the tumor is about 60% of its original size. We can also estimate the critical radius needed to constitute a spheroid,  $R_c$ , by assuming the critical cell number to be O(100) cells. Using this information together with  $R_{min}$ , we can predict the largest tumor that a single dose of a particular drug can eradicate as

$$R_{\text{max}} \sim \frac{R_{\text{c}}}{(\beta C)^{1/3\xi_2}} \frac{e^{1/3\xi_2(1-\beta C)}}{e^{1/3\xi_2(1-\beta C)}}.$$
 (25)

#### 3.1.3. Effect of administration schedule

The dosing strategy can effect the drug concentrations in the blood, normal tissue and tumor. Fig. 1 shows a comparison between a bolus injection and continuous infusion of the same amount of drug over an 8 h period. Here we assume  $R_c \approx 0.02$  cm. In each case the drug is administered every seven days and the tumor radius is measured at one week intervals. The results show that tumor responds slightly better to the bolus injection strategy giving a cure three weeks sooner than continuous infusion. However, because the drug levels in the blood are significantly higher for bolus administration than for continuous infusion, the decrease in toxic effects associated with continuous infusion may make it the preferred strategy.

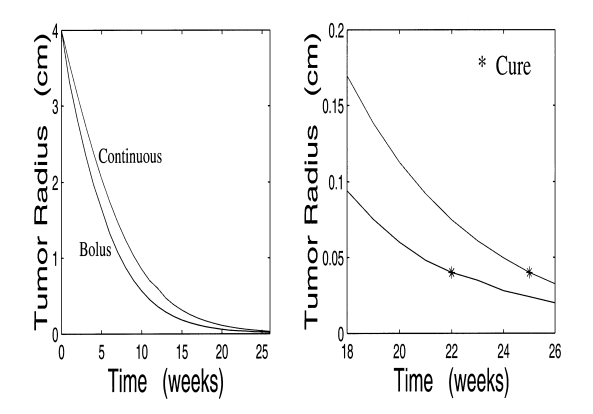


Fig. 1. Diagrams comparing the tumor's response to the delivery, over an 8 h period, of equal amounts of drug administered either by a bolus injection or by continuous infusion. The bolus injection leads to a rapid reduction of the tumor, with a cure effected after 22 weeks rather than 25 weeks for continuous infusion. Parameter values: see Table 1.

#### 3.1.4. Effect of different vascular distributions on tumor response to therapy

If the tumor is entirely avascular,  $\Gamma=0$ , and the drug can only enter the tumor via diffusion from the surrounding normal tissue. In this case, it takes longer for the drug to accumulate in the tumor, and hence, the response is delayed. Equally, no drug is able to escape back into the vasculature, so that the positive effects of therapy may eventually outweigh those of constant blood–tissue transfer as seen in Fig. 2.

In order to investigate the effect of a spatially dependent blood-tissue transfer function we now take

$$\Gamma(r) = \Gamma H(r - R_{\mathrm{V}}) = \begin{cases} \Gamma, & R_{\mathrm{V}} < r < R, \\ 0, & 0 < r < R_{\mathrm{V}}, \end{cases}$$

in Eq. (17). This localizes the vasculature to the outer edge of the tumor, in an annulus of width  $R-R_{\rm V}$ , leaving the inner core entirely avascular. Note that with this choice of  $\Gamma(r)$  there is no vascular exchange when the tumor is sufficiently small (i.e.  $0 < R < R_{\rm V}$ ). The results presented in Fig. 2 demonstrate the effect of incorporating this function with  $R_{\rm V}=0.32$  cm into Eq. (1). When the same parameter values are used, simulations show that when the bloodtissue transfer depends on radial position, the tumor's response is superior to that of an avascular tumor.

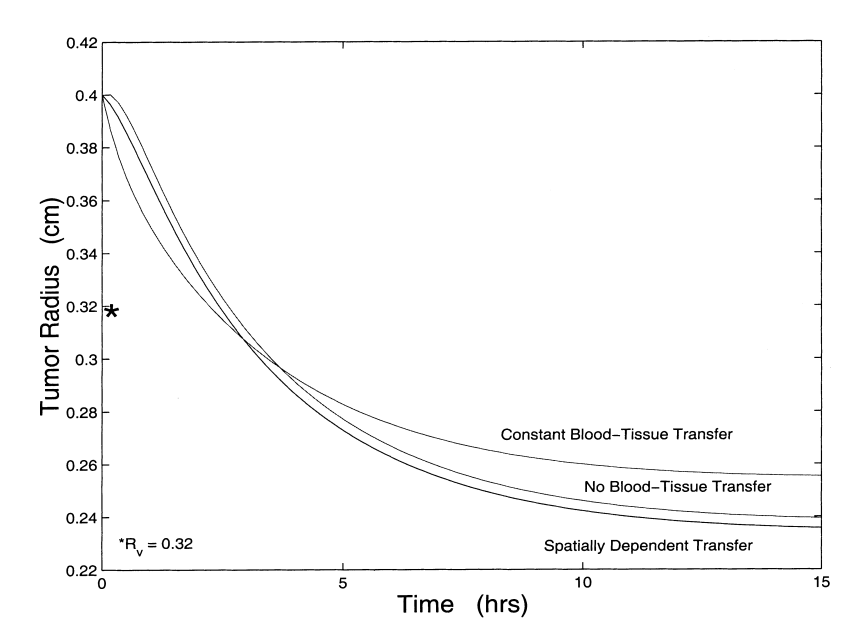


Fig. 2. Sketch showing how the presence of a vasculature exchange affects the tumor's response to therapy. Initially the model with constant blood–tissue transfer yields the most rapid reduction in the tumor volume. However, for later times the model with spatially-dependent blood–tissue transfer gives rise to the largest reduction in tumor volume. Parameter values: see Table 1;  $R_V = 0.32$  cm denotes the dimensional tumor radius at which a vascular first appears for the model with spatially-varying blood–tissue transfer.

#### 4. Two cell types

We now re-introduce the second cell population into our model (q > 0) and assume that these cells are less responsive to the therapy. Being independent of the cell densities, the intratumoral drug profiles are unaltered by the re-introduction of q into the model. Recalling that cellular diffusion can be neglected with respect to the convective motion, we fix  $\sigma_1 = \sigma_2 = 0$  in Eqs. (12) and (13) and focus on the following non-dimensional equations which describe the evolution of the p-cells, the cell velocity and the tumor radius:

$$\frac{\partial p}{\partial t} + \frac{1}{r^2} \frac{\partial}{\partial r} (r^2 u p) = p \left( 1 - \frac{p}{\delta_1} \right) - \frac{\beta_1 d p}{\gamma_1 + p},\tag{26}$$

$$\frac{1}{r^2} \frac{\partial}{\partial r} (r^2 u) = p \left( 1 - \frac{p}{\delta_1} \right) + \alpha_2 q \left( 1 - \frac{q}{\delta_2} \right) - \frac{\beta_1 dp}{\gamma_1 + p} - \frac{\beta_2 dq}{\gamma_2 + q}, \tag{27}$$

$$\frac{\mathrm{d}R}{\mathrm{d}t} = u(R, t),\tag{28}$$

where  $\alpha$  is now equal to the growth rate of the susceptible cell type,  $\alpha_1$ . As in Section 3, the drug concentration d(r,t) is known in terms of R(t),  $d_N(t)$  and  $d_B(t)$  from Eq. (20). We remark also that, by incompressibility, the density of the q-cells is known in terms of the density of the p-cells: q = 1 - p.

#### 4.1. Analysis

In order to make analytical progress, the following simplifying assumptions are made:

$$\delta_i \gg 1$$
,  $\gamma_i \gg 1$ ,  $\beta_i \gg 1$  with  $\frac{\beta_i}{\gamma_i} \sim O(1)$ .

The first assumption ensures exponential growth of the tumor when no drug is present. The latter assumptions mean that the response of both cell types to the treatment is linear. Under these assumptions, and with q = 1 - p, Eqs. (26) and (27) reduce to

$$\frac{\partial p}{\partial t} + \frac{1}{r^2} \frac{\partial}{\partial r} (r^2 u p) = p \left( 1 - \frac{\beta_1}{\gamma_1} d \right), \tag{29}$$

$$\frac{1}{r^2}\frac{\partial}{\partial r}(r^2u) = p\left(1 - \alpha_2 - \frac{\beta_1 d}{\gamma_1} + \frac{\beta_2 d}{\gamma_2}\right) + \left(\alpha_2 - \frac{\beta_2}{\gamma_2}d\right),\tag{30}$$

$$\frac{\mathrm{d}R}{\mathrm{d}t} = u(R, t). \tag{31}$$

Now if the density of drug-resistant cells is small we introduce the small parameter  $0 < \eta \ll 1$  and seek solutions of the form

$$p = 1 - \eta \tilde{p}, \quad q = \eta \tilde{p}, \quad u = u_0 + \eta u_1, \quad R = R_0 + \eta R_1.$$
 (32)

Substituting (32) into (29) and (30) and equating to zero terms of  $O(\eta^n)$  enables us to determine  $u_0, u_1, R_0, R_1$  and  $\tilde{p}$ . Of particular interest is establishing conditions under which the drug resistant population grows or decays.

#### 4.1.1. Drug-free growth

With d = 0 substitution of (32) into Eqs. (29)–(31) leads to the following equations:

$$O(1): \frac{1}{r^2} \frac{\partial}{\partial r} (r^2 u_0) = 1,$$

$$\frac{dR_0}{dt} = u_0(R_0, t),$$
(33)

$$O(\eta): \frac{\partial \tilde{p}}{\partial t} + \frac{1}{r^2} \frac{\partial}{\partial r} (r^2 u_0 \tilde{p}) = \alpha_2 \tilde{p},$$

$$\frac{1}{r^2} \frac{\partial}{\partial r} (r^2 u_1) = (1 - \alpha_2) \tilde{p},$$

$$\frac{dR_1}{dt} = u_1(R_0, t) + R_1 \frac{\partial u_0}{\partial r} (R_0, t).$$
(34)

Assuming that  $\tilde{p}(r,0) = \tilde{p}_0$  and that R(t=0) = 1, the solutions of (33) and (34) are

$$u_0(r,t) = \frac{r}{3}, \quad \tilde{p}(r,t) = \tilde{p}_0 e^{-(1-\alpha_2)t}, \quad u_1(r,t) = \frac{\tilde{p}_0(1-\alpha_2)r}{3} e^{-(1-\alpha_2)t}, \qquad 0 < r < e^{t/3} = R_0(t).$$
(35)

As expected, Eq. (35) demonstrates that when d = 0 the perturbations decay over time if  $\alpha_2 < 1$ , i.e. if the drug resistant population proliferates less rapidly than the drug-sensitive population. In this case, the fraction of resistant cells ultimately vanishes, leaving only the original dominant cell type. The elimination of the resistant cell type is due to the fact that we consider a small perturbation from the one cell type case and assume slower proliferation of the sensitive cells. Also, in this model there is no direct effect of one cell type on the other. Such coupling would certainly alter the population dynamics and will be the subject of future work.

#### 4.1.2. Continuous infusion of the drug, $d(r,t) = d_c$

Assuming constant drug concentration within the tumor mass results in the following equations:

$$O(1): \frac{1}{r^2} \frac{\partial}{\partial r} (r^2 u_0) = 1 - \frac{\beta_1}{\gamma_1} d_c, \frac{dR_0}{dt} = u_0(R_0, t),$$
 (36)

$$O(\eta): \frac{\partial \tilde{p}}{\partial t} + \frac{1}{r^2} \frac{\partial}{\partial r} (r^2 u_0 \tilde{p}) = \left(\alpha_2 - \frac{\beta_2}{\gamma_2} d_{\rm c}\right) \tilde{p},$$

$$\frac{1}{r^2} \frac{\partial}{\partial r} (r^2 u_1) = \left[\left(\alpha_2 - \frac{\beta_2}{\gamma_2} d_{\rm c}\right) - \left(1 - \frac{\beta_1}{\gamma_1} d_{\rm c}\right)\right] \tilde{p},$$

$$\frac{dR_1}{dt} = u_1(R_0, t) + R_1 \frac{\partial u_0}{\partial r} (R_0, t).$$
(37)

Assuming, as above, that  $\tilde{p}(r,0) = \tilde{p}_0$  and R(t=0) = 1, the solutions of (36) and (37) are

$$u_{0}(r,t) = \frac{r}{3} \left( 1 - \frac{\beta_{1}}{\gamma_{1}} d_{c} \right),$$

$$\tilde{p}(r,t) = \tilde{p}_{0} \exp \left\{ \left[ d_{c} \left( \frac{\beta_{1}}{\gamma_{1}} - \frac{\beta_{2}}{\gamma_{2}} \right) - (1 - \alpha_{2}) \right] t \right\},$$

$$u_{1} = \frac{\tilde{p}_{0} \left[ \left( \alpha_{2} - \frac{\beta_{2}}{\gamma_{2}} d_{c} \right) - \left( 1 - \frac{\beta_{1}}{\gamma_{1}} d_{c} \right) \right] r}{3} \exp \left\{ \left[ d_{c} \left( \frac{\beta_{1}}{\gamma_{1}} - \frac{\beta_{2}}{\gamma_{2}} \right) - (1 - \alpha_{2}) \right] t \right\},$$

$$0 < r < R_{0}(t) = e^{\left( 1 - \frac{\beta_{1}}{\gamma_{1}} d_{c} \right) t/3}.$$
(38)

From (38) we see that perturbations in the cell density will grow if

$$d_{\rm c} > \frac{1 - \alpha_2}{(\beta_1/\gamma_1) - (\beta_2/\gamma_2)}$$

and decay otherwise. Also, the tumor will regress, to first-order, if  $d_c > \gamma_1/\beta_1$ , but perturbations will decay if

$$d_{\rm c}<\frac{1-\alpha_2}{(\beta_1/\gamma_1)-(\beta_2/\gamma_2)}.$$

Now the two limiting curves which mark the transition between growth and decay of the perturbations intersect when  $\beta_2 = \beta^* = \alpha_2 \beta_1 \gamma_2 / \gamma_1$  giving a threshold for the drug's effect on the resistant cell population.

To be physically realistic we will assume that  $d_c$ ,  $\alpha_2$ ,  $\beta_2 > 0$ . Another common assumption in what follows is that  $(\beta_2/\gamma_2) < (\beta_1/\gamma_1)$ , i.e. the q-cells are less sensitive to the drug than the p-cells. Figs. 3 and 4 are bifurcation diagrams showing how the behavior of the tumor, as predicted by the asymptotic theory above, is affected by the parameters  $\beta_2$  and  $d_c$ . The results presented in Fig. 3 correspond to the case  $\alpha_2 < 1$  so that the drug-resistant q-cells proliferate less rapidly than the drug-sensitive cells. The diagram can be used to identify optimal regions of parameter space for successful treatment, with treatment being regarded as successful if the tumor radius is decreasing  $(R_0)$  and  $(R_1)$  and the drug resistant population  $(R_0)$  and  $(R_1)$  and the drug resistant population  $(R_0)$  is decaying  $(R_0)$ .

Fig. 3 shows that if  $\beta_2 < \beta^*$ , then there is no level of drug that will result in a cure. However as  $d_c$  increases from zero with  $\beta_2 > \beta^*$  a region is created in which the tumor's radius is decreasing to leading order, as are the perturbations in tumor radius and resistant cell density, i.e. this region gives rise to a cure.

In Fig. 4,  $\alpha_2 > 1$  which means that the drug-resistant population proliferates more rapidly than the drug-sensitive population. In this case,  $\beta_2 = \beta^* = \alpha_2 \beta_1 \gamma_2 / \gamma_1$  contradicts the assumption that the q-cells are less sensitive to the drug than the p-cells  $((\beta_2/\gamma_2) < (\beta_1/\gamma_1))$ . This means that the key curves do not intersect and there is no optimal parameter regime for successful treatment.

#### 4.1.3. Response of a small tumor

When  $0 < R \ll 1$ , the concentration of drug in the tumor will be equal to the concentration of drug in the normal tissues (i.e.  $d(r,t) = d_N(t)$ ). We know that the long time behavior of the drug in

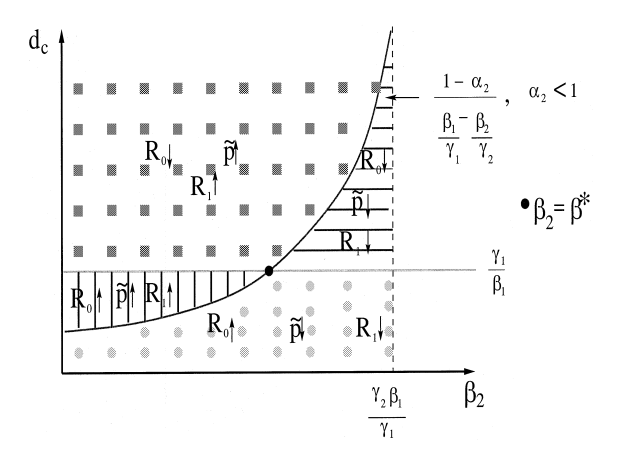


Fig. 3. Bifurcation diagram for the case  $\alpha_2 < 1$  showing the decomposition of  $(\beta_2, d_c)$  parameter space into distinct regions according to the tumor's response to the drug. Optimal regions of parameter space occur when both the tumor radius and the perturbations to the drug-sensitive cell density are decreasing (i.e.  $R \downarrow$  and  $\tilde{p} \downarrow$ ).

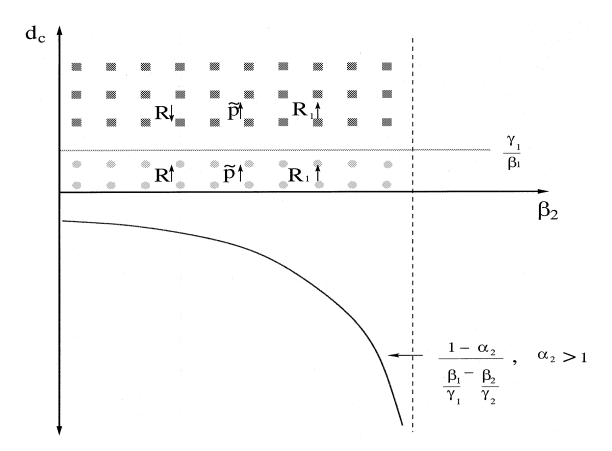


Fig. 4. Bifurcation diagram showing that when  $\alpha_2 > 1$  the linear theory predicts that there is no longer an optimal parameter regime for successful treatment: either the tumor radius decreases and the perturbation to the drug sensitive cell density increases or conversely.

the normal tissue is exponential elimination, that is  $d_N(t) \sim C e^{-\xi_2 t}$ . Using this information we find that for  $0 < r < R_0(t) = \exp[(t - \frac{\beta_1}{\gamma_1} \int d_N(\tau) d\tau)/3]$ :

$$u_{0}(r,t) = \frac{r}{3} \left( 1 - \frac{\beta_{1}}{\gamma_{1}} d_{N} \right) = \frac{r}{3} \left( 1 - \frac{\beta_{1}}{\gamma_{1}} C e^{-\xi_{2}t} \right),$$

$$\tilde{p}(r,t) = \tilde{p}_{0} \exp \left\{ - (1 - \alpha_{2})t - \left( \frac{\beta_{1}}{\gamma_{1}} - \frac{\beta_{2}}{\gamma_{2}} \right) \int^{t} d_{N}(\tau) d\tau \right\},$$

$$u_{1}(r,t) = \left[ \left( \alpha_{2} - \frac{\beta_{2}}{\gamma_{2}} d_{N} \right) - \left( 1 - \frac{\beta_{1}}{\gamma_{1}} d_{N} \right) \right] \left( \frac{\tilde{p}(r,t)r}{3} \right).$$

$$(39)$$

Therefore to first-order, the system behaves identically as in the one cell type case. Perturbations to these first-order solutions will grow until

$$t^* \approx \frac{C((\beta_1/\gamma_1) - (\beta_2/\gamma_2))}{\xi_2(1-\alpha_2) + C(\beta_1/\gamma_1) - C(\beta_2/\gamma_2)}.$$

When  $t = t^*$ , perturbations begin to decay implying that the tumor will regress for a short time before growth resumes.

#### 5. Numerical simulations of full model

In this section, we present numerical results obtained for the full system of Eqs. (23)–(25) and (13) that govern vascular tumor evolution when both drug sensitive and drug resistant cell types are present. The numerical results are obtained by mapping the moving boundary to the unit interval and this is achieved by transforming the spatial variable to  $r^* = r/R(t)$ . The transformed equations are then discretized using an implicit finite difference scheme [19]. The numerical results presented below show how the introduction of a drug resistant cell type affects the tumor's response to the chemotherapeutic agent and, in particular, the time to cure. Unless otherwise noted, the parameters not given in Table 1 have the following values:  $\alpha_2 = 0.9$ ,  $\gamma_i = 1.0$ ,  $\delta_i = 100$ .

#### 5.1. Effect of resistant cell population on tumor evolution

As the results of Fig. 5 demonstrate, the effects of the drug resistant population on the tumor's response to a bolus injection of drug is marked. Fig. 5 shows the temporal evolution of the tumor radius when both cell types are present at varying densities, and all other parameters are held fixed at the baseline values listed in Table 1. It is interesting to note that the speed of recovery is virtually independent of the initial density of drug sensitive and drug resistant cells. In each case the qualitative behavior of the tumor is the same: there is a period of tumor regression during which the drug is acting and this is followed by re-growth of the tumor. However, because tumor reduction is significantly decreased when a resistant cell type is present, the drug is successively

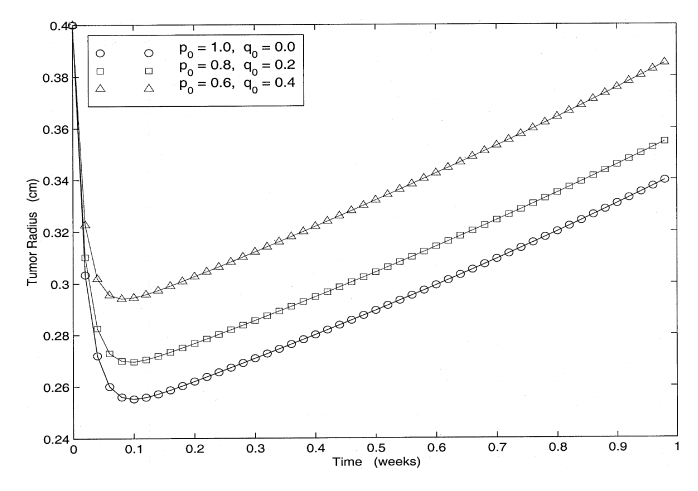


Fig. 5. Sketches showing how the evolution of the tumor radius changes when a resistant cell type is present at varying densities. Parameters not given in Table 1 have the following values:  $\alpha_2 = 0.9$ ,  $\gamma_i = 1.0$ ,  $\delta_i = 100$ .

less effective as the proportion of resistant cells increases. This reduction in drug efficacy may be assessed in two ways: by measuring the minimum tumor radius  $R_{\min}$  and the time  $t_{\min}$  at which this minimum is attained.

Fig. 6 shows how  $R_{\min}$  (cm) and  $t_{\min}$  (h) vary with initial density of drug sensitive cells,  $p_0$  following a bolus injection of drug. As the proportion of drug sensitive cells increases,  $R_{\min}$  decreases and the time to attain this minimum value increases. We note also that when there are no resistant cells present ( $p_0 = 1$ ), the simulations predict  $t_{\min} = 17.0$  h which correlates well with the theoretical estimate of 17.4 h derived in Section 3 (see Eq. (24)).

Fig. 7 indicates how, for a typical simulation of a bolus injection of drug, the distribution of the drug-sensitive population changes over time (here  $p_0 = 0.75$ ,  $q_0 = 0.25$ ) and suggests that the profiles are settling to a spatially-mixed steady state for which  $p(r^*,t) = p(t) \ \forall \ r^* \in (0,1)$ . The initial cell death at the boundary of the tumour is due to the fact that drug levels at the boundary are equal to those of the normal tissue.

Fig. 8 shows how the average cell density in the tumor  $(\int_0^{R(t)} p(r,t)r^2 dr)$  changes with time as we vary (a) the initial cell densities, (b) the drug's effect on the sensitive cell type, (c) the vascular permeability,  $\Gamma$  and (d) the drug's blood clearance rate. In Fig. 8(b)–(d) the initial cell density is held fixed at  $p_0 = 0.75$ . Again we have simulated a bolus injection of the chemotherapeutic agent. From these figures we observe that threefold changes in the drug's effect on the sensitive cell type can have remarkable effects on the cell density, whereas 1000-fold changes in the vascular permeability have only a limited effect. Such predictions provide useful information for the design of new therapies by helping to identify those physical parameters which have the largest impact on the tumor's development.

## 5.2. Effect of vascular distribution on chemotherapeutic response of tumor with resistant cell population

In order to investigate the effect of a spatially dependent blood–tissue transfer function when a drug resistant population of cells inhabits the tumor we take, as before

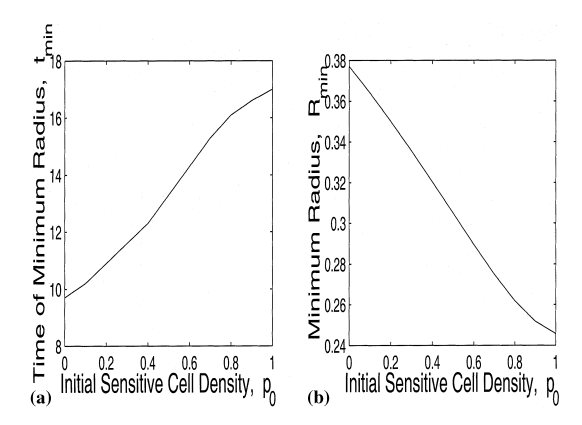


Fig. 6. Diagrams showing how (a) the time at which the minimum tumor radius  $t_{\min}$  (b) and (b) the corresponding value of the minimum tumor radius  $R_{\min}$  (cm) vary with the initial density of the drug sensitive cells  $p_0$ . Whilst  $t_{\min}$  increases with  $p_0$  the corresponding value of  $R_{\min}$  decreases. Parameters not given in Table 1 have the following values:  $\alpha_2 = 0.9$ ,  $\gamma_i = 1.0$ ,  $\delta_i = 100$ .

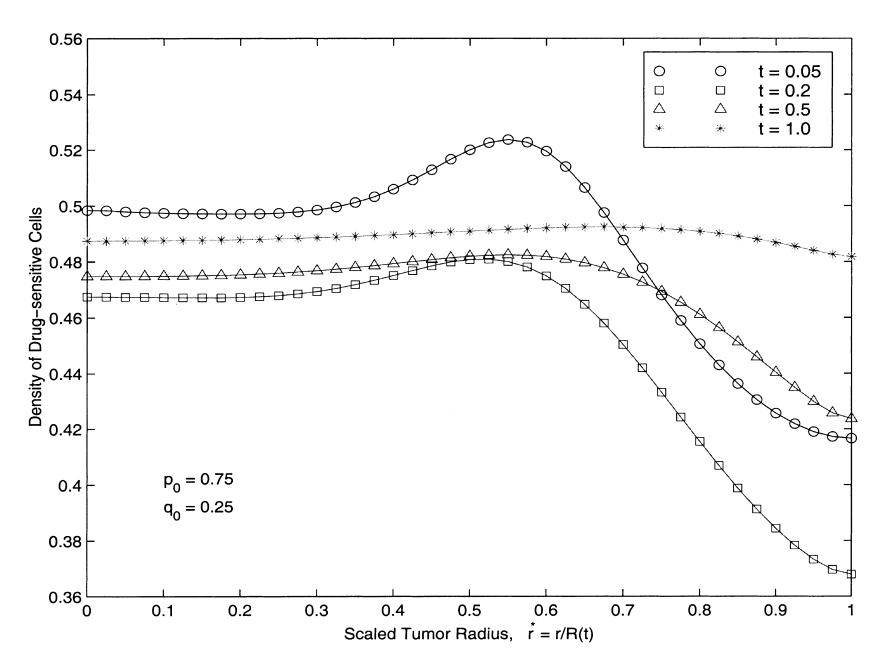


Fig. 7. Sequence of plots showing how the spatial distribution of the drug sensitive cells within the tumor changes over time. As t increases the population tends to a spatially-uniform profile. Parameters not given in Table 1 have the following values:  $\alpha_2 = 0.9$ ,  $\gamma_i = 1.0$ ,  $\delta_i = 100$ .

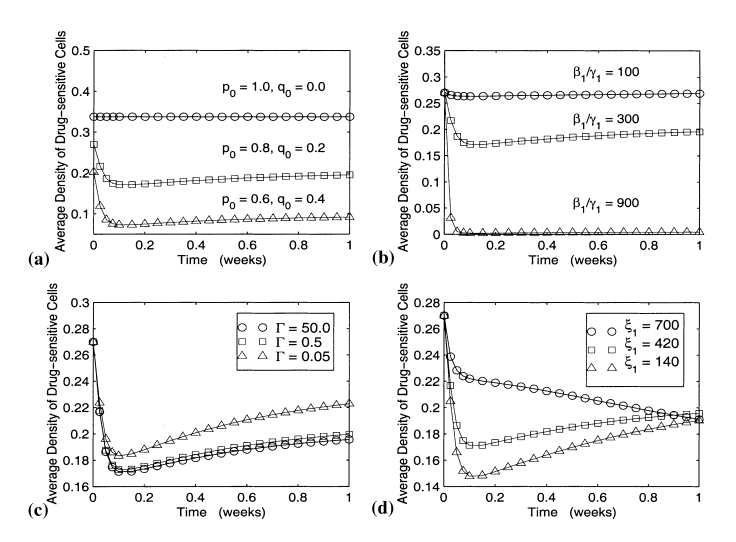


Fig. 8. Temporal changes in the average drug sensitive cell density within the tumor as we vary (a) the initial cell densities, (b) the drug's effect on the sensitive cell type, (c) the vascular permeability,  $\Gamma$ , and (d) the drug's initial blood clearance rate. In Fig. 8(b)–(d) the initial cell density is held fixed at  $p_0 = 0.75$ . Parameter values: see Table 1 and text.

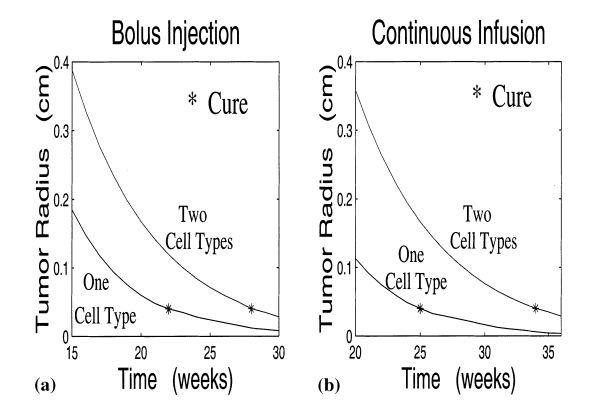


Fig. 9. Sequence of diagrams comparing the tumor's response to (a) bolus injection and (b) continuous infusion in the presence and absence of a resistant cell type. Parameters not given in Table 1 have the following values:  $\alpha_2 = 0.9$ ,  $\gamma_i = 1.0$ ,  $\delta_i = 100$ .

$$\Gamma(r) = \Gamma H(r - R_{\mathrm{V}}) = \begin{cases} \Gamma, & R_{\mathrm{V}} < r < R, \\ 0, & 0 < r < R_{\mathrm{V}}, \end{cases}$$

in Eq. (17). With  $R_V = 0.32$  in Eq. (1),  $p_0 = 0.75$  and all other parameters unchanged, we find that the tumor's response is optimal when only the periphery is vascularized. Since the resulting profile for R(t) is almost identical to that presented in Fig. 2, when there are no resistant cells present, the results are not presented here.

#### 5.3. Effect of resistant cell type on time to cure

The addition of a resistant cell type can markedly alter the time to cure when either a bolus injection or a continuous infusion of a single chemotherapeutic agent is administered on a weekly basis. Fig. 9 shows how the addition of a small fraction of resistant cells can affect the tumor's response to therapy: when a bolus is applied to a tumor containing only drug sensitive cells it is effectively eliminated after approximately 22 weeks (see Fig. 1). By contrast when 20% of the cancer cells are resistant, it takes about 28 weeks to cure the cancer. Fig. 1 shows that continuous infusion results in a cure at approximately 25 weeks when only drug sensitive cells are present. However when a small population of drug resistant cells also inhabits the tumor, Fig. 9 shows that the time to cure can increase by over two months.

#### 6. Discussion

In this paper we have developed a mathematical model that describes the response of a spherically-symmetric vascular tumor, which contains two types of cells, to chemotherapeutic treatment. The model is formulated as a system of partial differential equations that describe the evolution of the drug and cell populations within the tumor. The tumor radius is tracked by introducing a velocity field to describe cell motion generated by the balance between cell proliferation and death.

Using a combination of numerical and analytical techniques we were able to use the model to investigate the tumor's response to various chemotherapeutic strategies (e.g. continuous infusion and bolus injection) and to contrast the behavior of tumors containing semi drug resistant populations.

When the tumor consisted of one cell type, drug sensitive it was possible to derive an analytical estimate of the minimum tumor radius attained after a bolus injection of the drug. It was also possible to estimate the time at which tumor re-growth would resume. By assuming further that there was a critical radius necessary to constitute a spheroid we were able to derive a formula for the largest such tumor that could be eradicated by a bolus injection.

The emergence of drug resistance in a previously drug-sensitive tumor is thought to be one of the major barriers to effective chemotherapeutic treatment [20]. Biochemical or phenotypic resistance may arise in cells via spontaneous mutation [21] or be acquired as a result of exposure to the drug [22]. Notable differences in the tumor's response to therapy were observed when a second, drug resistant cell population was incorporated into the model. Although the speed of resumed tumor growth was virtually independent of the initial resistant cell density; the minimum radius achieved is significantly increased and the time of resumed growth is decreased as  $q_0$  increases. We also found that a tumor with a well-vascularized periphery and large avascular center responds best to treatment in the presence and absence of a drug resistant cell type.

Using our mathematical model we were also able to show that the drug administration strategy can have a significant impact on the time to cure (where cure is possible). For example, numerical simulations of the model equations showed that bolus injection and continuous infusion of the drug resulted in similar times to cure of a tumor containing only one type of drug sensitive cells. This implies that continuous infusion may be the preferred treatment due to lower toxicity in the circulating blood. By contrast, when the tumor contains a drug resistant population, continuous infusion significantly increases the time to cure, making bolus injection the preferred strategy. This result indicates clearly the need to tailor treatment strategies to specific tumors.

The modeling framework that we have developed and our preliminary findings lead naturally to several possibilities for extended studies. A couple of these modifications are discussed below.

#### 6.1. More sophisticated chemotherapeutic approaches

The model studied in this paper considers the response of tumors to traditional chemotherapy. It would be interesting to compare and contrast these results with a model that has been extended to include other chemotherapeutic approaches. For example, direct drug targeting where the drug is bound to an antibody and this conjugate must bind to cells in order to initiate cell death. There are also very promising two-step approaches to chemotherapy in which an antibody–enzyme conjugate followed by a prodrug is administered. The antibody conjugate binds to tumor cells and the enzyme converts the prodrug to an active cytotoxic agent [23,24]. A mathematical investigation into the effectiveness of these three treatment strategies in homogeneous or multi-cell type tumors could provide insight into the conditions for which one strategy is better than another.

#### 6.2. Inclusion of complex cellular and vascular dynamics

In the present model the drug concentration evolves independently of the tumor cell populations and coupling between the two cell populations is weak, being mediated only by the cell

velocity u. It would be useful to investigate the effects of competition between cell types by coupling p and q via their proliferation rates ( $F_p = F_p(p,q)$  and  $F_q = F_q(p,q)$  in Eqs. (2) and (3)). The equation for drug concentration in the tumor could also be modified to describe its degradation by the tumor cells. In addition, since most chemotherapeutic agents are designed to act on metabolically active or rapidly dividing cells, it may be necessary to introduce cell-cycle specific terms into the model framework as in [25].

Experimental studies suggest that two different mechanisms contribute to cell loss within a tumor: apoptosis which is the programmed death of a cell and necrosis which is the micro-environment induced death of a cell. An investigation of these two distinct cell loss mechanisms appears in [26]. There is no mention in the present model of necrotic cell death, hypoxia, rate of progression through the cell cycle or cell cycle arrest. Including these phenomena could have significant effects on the results presented here.

Angiogenesis, the formation of new blood vessels, appears to be one of the crucial steps in a tumor's transition from small and harmless to large and malignant [27,28]. The work of Judah Folkman and his coworkers [27,29] has sparked considerable interest in anti-angiogenic treatments which aim to prevent metastases and rapid tumor growth by manipulating the tumor vasculature. Where traditional cancer treatment attempts to remove or eradicate the tumor from the body, anti-angiogenic therapy attempts to shrink tumors and prevent them from growing by limiting their blood supply. Anti-angiogenic drugs stop new vessels from forming and breaks up the existing vascular network that feeds the tumor. Anti-angiogenic drugs have been approved for use on humans and many more are now in pre-clinical trials. In addition, several potential inhibitors such as angiostatin and endostatin are being studied in research laboratories, as well as by pharmaceutical and biotechnology companies. Whilst in the present paper the effect that the drug has on the tumor vasculature has been neglected, the dynamics of vascular shunting, collapse, and re-growth are also interesting directions for future work.

#### 6.3. Non-spherical geometries

There are two natural ways in which to alter the geometry of the problem we have addressed. The first approach corresponds to modeling the tumour as a cylinder. This approach considers tumour cords or cuffs where the tumour grows radially outward from a central blood vessel. Essentially, the same mathematical model could be studied, but with a different geometry and different assumptions regarding its symmetry; for example, it would be natural to impose radial symmetry initially.

The second approach is to consider how the radially symmetric solutions respond to asymmetric perturbations. Due to the form of the model equations the natural choice for the perturbations are spherical harmonics. Any modes that are excited indicate how the tumour may invade into its surrounding tissues. Several authors have studied how these types of perturbations will effect the growth of multicellular spheroids [7,30–32]. To our knowledge there has not been an investigation into how treatment would be affected by such an invading tumour. This open question could also be an area of future study.

The modeling framework that we have developed has been able to predict the response of vascular tumors with two distinct clonal populations to chemotherapeutic treatment. The formulation of the model is general enough that more of the tumor physiology can be included and

more sophisticated treatment strategies can be investigated. The mathematical model provides a means for determining the most advantageous dosing strategy for tumor reduction, and suggests future experimental directions which can lead to improved protocols for chemotherapeutic treatment.

#### Appendix A. Plasma and normal tissue dynamics

The standard pharmacokinetic equations based on a two compartment model for drug concentrations in a central compartment  $(d_B(t))$  consisting of the blood volume together with the extracellular fluid of highly perfused tissues of the body and a peripheral compartment formed by less perfused tissues  $(d_N(t))$  following a bolus injection are

$$\frac{\mathrm{d}d_B}{\mathrm{d}t} = -k_{12}d_B + k_{21}d_N - k_e d_B, 
\frac{\mathrm{d}d_N}{\mathrm{d}t} = k_{12}d_B - k_{21}d_N.$$
(A.1)

The parameters,  $k_{12}$  and  $k_{21}$  are rates of transfer from the blood to the tissues of the body and from the tissues back into the blood and  $k_e$  is the plasma clearance rate. A major assumption of this classical approach to compartmental modeling [36] is that the body can be resolved into compartments which do not necessarily correspond specific anatomic entities but to theoretical spaces postulated to account for experimental observation. The above system can be solved via Laplace transforms and has solutions of the form

$$d_B(t) = A e^{-\xi_1 t} + B e^{-\xi_2 t}$$
 and  $d_N(t) = C(e^{-\xi_2 t} - e^{-\xi_1 t}).$  (A.2)

The values for A, B,  $\xi_1$  and  $\xi_2$  are taken from a best fit to experimental blood clearance data and are used to calculate the actual pharmacokinetic parameters as follows [36]:

$$k_{e} = \frac{A+B}{(A/\xi_{1}) + (B/\xi_{2})},$$

$$k_{21} = \frac{A\xi_{2} + B\xi_{1}}{A+B},$$

$$k_{12} = \frac{AB}{(A+B)^{2}} \frac{(\xi_{2} - \xi_{1})^{2}}{k_{21}},$$

$$V_{1} = \frac{\text{dose}}{A+B},$$

$$V_{2} = V_{1} \frac{k_{12}}{k_{21}}.$$
(A.3)

The normal tissue coefficient, C, is related to these parameters as follows:

$$C = \sqrt{k_{12}^2 + 2k_{12}k_e + 2k_{12}k_{21} + k_e^2 - 2k_{21}k_e + k_{21}^2}/k_{12}.$$

Note, that the apparent volumes of the central and peripheral compartments,  $V_1$  and  $V_2$ , are computed in terms of the parameter of the system [36].

The blood dynamics change slightly when we consider the tumor as a separate compartment. Instead of (A.1) we now have

$$\frac{\mathrm{d}d_B}{\mathrm{d}t} = -k_{12}d_B + k_{21}d_N - k_e d_B - \Gamma(d_B - d(R(t), t)), 
\frac{\mathrm{d}d_N}{\mathrm{d}t} = k_{12}d_B - k_{21}d_N.$$
(A.4)

The boundary conditions for the amount of drug in the tumor tell us that  $d(R(t), t) = d_N(t)$  so that the changes in going from (A.1)–(A.4) result in only minor changes to the compartmental transfer coefficients. That is, the basic form of the solution is unchanged.

#### References

- [1] J.A. Adam, A mathematical model of tumor growth. ii: Effects of geometry and spatial uniformity on stability, Math. Biosci. 86 (1987) 183.
- [2] J.A. Adam, A mathematical model of tumor growth iii: Comparison with experiment, Math. Biosci. 86 (1987) 213.
- [3] J.A. Adam, S.A. Maggelakis, Diffusion regulated growth characterisites of a spherical prevascular carcinoma, Bull. Math. Biol. 52 (1990) 549.
- [4] H.M. Byrne, M.A.J. Chaplain, Growth of non-necrotic tumors in the presence and absence of inhibitiors, Math. Biosci. 130 (1995) 151.
- [5] H.M. Byrne, M.A.J. Chaplain, Growth of necrotic tumors in the presence and absence of inhibitors, Math. Biosci. 135 (1996) 187.
- [6] H.P. Greenspan, Models for the growth of a solid tumor by diffusion, Stud. Appl. Math. 52 (1972) 317.
- [7] H.P. Greenspan, On the growth and stability of cell cultures and solid tumors, J. Theor. Biol. 56 (1976) 229.
- [8] S.A. Maggelakis, J.A. Adam, Mathematical model of prevascular growth of a spherical carcinoma, Math. Comput. Modelling 13 (1990) 23.
- [9] J.P. Ward, J.R. King, Mathematical modeling of avascular-tumor growth, IMA J. Math. Appl. Med. Biol. 14 (1997) 39.
- [10] J. Folkman, M. Hochberg, Self-regulation of growth in three-dimensions, J. Exp. Med. 138 (1973) 743.
- [11] L.A. Kunz-Schughart, M. Kreutz, R. Kneuchel, Multicellular spheroids: a three- dimensional in vitro culture system to study tumor biology, Int. J. Eng. Path. 79 (1979) 1.
- [12] R.M. Sutherland, R.E. Durand, Growth and cellular characteristics of multicell spheroids, Recent Results Cancer Res. 95 (1994) 510.
- [13] M. Marusic, Z. Bajzer, S. Vuk-Pavlovic, J.P. Freyer, Tumor growth in vivo and as multicellular spheroids compared by mathematical models, Bull. Math. Biol. 56 (1994) 617.
- [14] P.D. Senter, J.D. Murray, Development and validation of a mathematical model to describe anti-cancer prodrug activation by antibody–enzyme conjugates, J. Theor. Med., in press.
- [15] T.L. Jackson, S.R. Lubkin, J.D. Murray, Theoretical analysis of conjugate localization in two-step cancer chemotherapy, J. Math. Bio. 39 (1999) 353.
- [16] L.E. Gerlowski, R.K. Jain, Microvascular permeability of normal and neoplastic tissues, Microvas. Res. 31 (1986) 288
- [17] R.K. Jain, Barriers to drug delivery in solid tumors, Sci. Am. 271 (1994) 58.
- [18] N.O. Siemers, D.E. Kerr, S. Yarnold, M. Stebbins, V.M. Vrudgyka, I. Hellstrom, K.E. Hellstrom, P.D. Senter, L49-sfv-β-lactamase a single chain anti-p97 antibody fusion protein, Bioconjugate Chem. 8 (1997) 510.
- [19] J. Crank, Free and moving boundary problems, OUP (1988).
- [20] B.G. Birkhead, E.M. Rankin, S. Gallivan, L. Dones, R.D. Rubens, A mathematical model of the development of drug resistance to cancer chemotherapy, Eur. J. Cancer Clin. Oncol. 23 (1987) 1421.

- [21] J.H. Goldie, A.J. Coldman, A mathematical model for relating the drug sensitivity of tumors to their spontaneous mutation rate, Cancer Treat. Rep. 63 (1971) 1727.
- [22] D. Crowther, A rational approach to the chemotherapy of human malignant disease ii, Rit. Med. J. 4 (1974) 216.
- [23] K.D. Bagshawe, R.H.J. Begent, First clinical experience with ADEPT, Adv. Drug Delivery Rev. 22 (1996) 365.
- [24] D.E. Kerr, G.J. Schreiber, V.M. Vrudhula, H.P. Svensson, K.E. Hellstrom, P.D. Senter, Regressions and cures of melanoma xenografts following treatment with monoclonal antibody β-lactamase conjugates in combination with anticancer prodrugs, Cancer Res. 55 (1995) 3558.
- [25] Z. Agur, R. Arnon, B. Schechter, Reduction of cytotoxicity to normal tissues by new regimens of cell cycle phase specific drugs, Math. Biosci. 92 (1988) 1.
- [26] H.M. Byrne, M.A.J. Chaplain, Necrosis and apoptosis: distinct cell loss mechanisms in a mathematical model of avascular tumor growth, J. Theor. Med. 1 (1998) 223.
- [27] J. Folkman, Fighting cancer by attacking its blood supply, Sci. Am. (1996) 150.
- [28] D. Hanahan, J. Folkman, Patterns and emerging mechanisms of the angiogenic switch during tumorigenesis, Cell 86 (1996) 353.
- [29] M.S. O'Reilly, T. Boehm, Y. Shing, N. Fukai, G. Vasios, W.S. Lane, E. Flynn, J.R. Birkhead, J. Folkman, Endostatin: An endogenous inhibitor of angiogenesis and tumor growth, Cell 88 (1997) 277.
- [30] H.M. Byrne, S.A. Gourley, The role of growth factors in avascular tumour growth, Math. Comput. Modeling 26 (1997) 83.
- [31] H.M. Byrne, M.A.J. Chaplain, Free boundary value problems associated with the growth and development of multicellular spheroids, Eur. J. Appl. Math. 8 (1997) 639.
- [32] H.M. Byrne, A weakly nonlinear analysis of a model of avascular solid tumour growth, J. Math. Bio. 39 (1997) 59.
- [33] L.T. Baxter, F. Yuan, R.K. Jain, Pharamacokinetic analysis of the perivascular distribution of bifunctional antiboies and haptens: comparison with experimental data, Cancer Res. 52 (1992) 5838.
- [34] L.J. Nugent, R.K. Jain, Extravascular diffusion in normal and neoplastic tissues, Cancer Res. 44 (1984) 238.
- [35] M.S. Dordal, J.N. Winter, A.J. Atkinson, Kinetic analysis of p-glycoprotein-mediated doxorubicin efflux, J. Pharmacol. Exp. Ther. 263 (1992) 762.
- [36] D.J. Greenblatt, J. Koch-Weser, Drug therapy: clinical pharmacokinetics, NE J. Med. 293 (1975) 702.
- [37] R.K. Jain, Transport of macromolecules across tumor vasculature, Cancer Metastasis Rev. 6 (1987) 559.
- [38] J. Robert, A. Illiadia, B. Hoerniand, J. Cano, M. Durand, C. Lagarde, Pharamacokinetics of adrianmycin in patients with breast cancer: correlation between pharmacokinetic parameters and clinical short-term respons, Eur. J. Cancer Clin. Oncol. 18 (1982) 739.